

Bonding Trends of Thiosemicarbazones in Mononuclear and Dinuclear Copper(I) Complexes: Syntheses, Structures, and Theoretical Aspects

Tarlok S. Lobana,^{*,†} Rekha,[†] R. J. Butcher,[‡] A. Castineiras,[§] E. Bermejo,[§] and Prasad V. Bharatam^{||}

Department of Chemistry, Guru Nanak Dev University, Amritsar 143 005, India, Department of Medicinal Chemistry, National Institute of Pharmaceutical Education and Research (NIPER), SAS Nagar, Punjab 160062, India, Department of Chemistry, Horward University, Washington, D.C. 20059, and Departamento de Química Inorganica, Facultad de Farmacia, Universidad de Santiago, 15782 Santiago, Spain

Received June 22, 2005

Reactions of copper(I) halides with a series of thiosemicarbazone ligands (Htsc) in the presence of triphenylphosphine (Ph₃P) in acetonitrile have yielded three types of complexes: (i) monomers, [CuX(η^1 -S-Htsc)(Ph₃P)₂] [X, Htsc = I (**1**), Br (**2**), benzaldehyde thiosemicarbazone (Hbtsc); I (**5**), Br (**6**), Cl (**7**), pyridine-2-carbaldehyde thiosemicarbazone (Hpytsc)], (ii) halogen-bridged dimers, [Cu₂(μ_2 -X)₂(η^1 -S-Htsc)₂(Ph₃P)₂] [X, Htsc = Br (**3**), Hbtsc; I (**8**), furan-2-carbaldehyde thiosemicarbazone (Hftsc); I (**11**), thiophene-2-carbaldehyde thiosemicarbazone (Httsc)], and (iii) sulfur-bridged dimers, [Cu₂X₂(μ_2 -S-Htsc)₂(Ph₃P)₂] [X, Htsc = Cl (**4**), Hbtsc; Br (**9**), Cl (**10**), pyrrole-2-carbaldehyde thiosemicarbazone (Hptsc); Br (**12**), Httsc]. All of these complexes have been characterized with the help of elemental analysis, IR, ¹H, ¹³C, or ³¹P NMR spectroscopy, and X-ray crystallography (**1**–**12**). In all of the complexes, thiosemicarbazones are acting as neutral S-donor ligands in η^1 -S or μ_2 -S bonding modes. The Cu...Cu separations in the Cu(μ_2 -X)₂Cu and Cu(μ_2 -S)₂Cu cores lie in the ranges 2.981(1)–3.2247(6) and 2.813(1)–3.2329(8) Å, respectively. The geometry around each Cu center in monomers and dimers may be treated as distorted tetrahedral. Ab initio density functional theory calculations on model monomeric and dimeric complexes of the simplest thiosemicarbazone [H₂C=N–NH–C(S)–NH₂, Htsc] have revealed that monomers and halogen-bridged dimers have similar stability and that sulfur-bridged dimers are stable only when halogen atoms are engaged in hydrogen bonding with the solvent of crystallization or H₂O molecules.

Introduction

Transition-metal and main group metal complexes of thiosemicarbazones have invited considerable interest for a variety of reasons such as variable bonding properties because of the presence of several donor sites, structural diversity, and pharmacological aspects.^{1–5} In neutral form,

thiosemicarbazones bind to a metal in *E* mode via generally an S donor atom (Scheme 1, **1a**), and after deprotonation at hydrazinic N²H hydrogen, they generally change into the *Z* form and bind to a metal in N³,S-chelating mode (**1b**).^{1–5} Cu^I has shown interesting bonding modes of sulfur in its interaction with heterocyclic thioamides, and a variety of complexes of variable nuclearity have been reported.⁶

Cu^{II} has formed several complexes with thiosemicarbazones,⁷ and some of them have shown biological activity and applications as radiopharmaceuticals.^{1–5,8} Thiosemicarbazones bearing a pyridine ring are known antitumor compounds and inhibitors of DNA synthesis,^{1–5} and this

* To whom correspondence should be addressed. E-mail: tarlokslobana@yahoo.co.in. Fax: 91-183-2-258820.

[†] Guru Nanak Dev University.

[‡] Horward University.

[§] Universidad de Santiago.

^{||} National Institute of Pharmaceutical Education and Research.

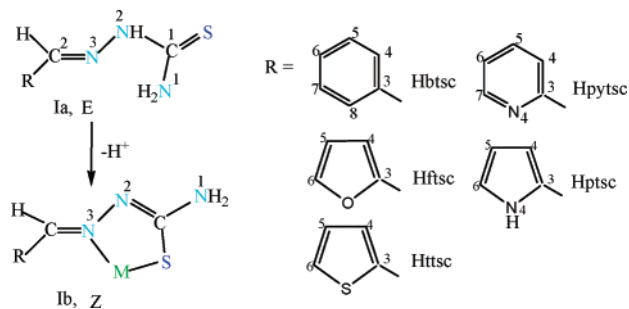
- (1) (a) Campbell, M. J. M. *Coord. Chem. Rev.* **1975**, *15*, 279. (b) Padhye, S. B.; Kauffman, G. *Coord. Chem. Rev.* **1985**, *63*, 127.
- (2) West, D. X.; Padhye, S. B.; Sonawane, P. B. *Struct. Bonding (Berlin, Ger.)* **1991**, *76*, 4.
- (3) West, D. X.; Liberta, A. E.; Padhye, S. B.; Chikate, R. C.; Sonawane, P. B.; Kumbhar, A. S.; Yerande, R. G. *Coord. Chem. Rev.* **1993**, *123*, 49.
- (4) Casas, J. S.; Garcia-Tasende, M. S.; Sordo, J. *Coord. Chem. Rev.* **2000**, *209*, 197.

- (5) Smith, D. R. *Coord. Chem. Rev.* **1997**, *164*, 575.

- (6) (a) Raper, E. S. *Coord. Chem. Rev.* **1985**, *61*, 115. (b) Raper, E. S. *Coord. Chem. Rev.* **1996**, *153*, 199. (c) Raper, E. S. *Coord. Chem. Rev.* **1994**, *129*, 91. (d) Raper, E. S. *Coord. Chem. Rev.* **1997**, *165*, 475.

- (7) Lobana, T. S.; Rekha; Butcher, R. J. *Transition Met. Chem.* **2004**, *29*, 291 and references cited therein.

Scheme 1



activity is attributed to their ability to inhibit the DNA topoisomerase II enzyme responsible for the regulation of the topology of DNA.⁸ The use of copper(II) thiosemicarbazone compounds in biological systems is bound to involve Cu^{II} reduction to Cu^I in the cells, and thus the stability of Cu^I species is crucial to the hypotoxic reactivity and biological activity of topo-II inhibitors. There are only limited reports on the structural chemistry of complexes of thiosemicarbazones with Cu^I.^{1–5,7,9–13} The main reason for the lack of copper(I) thiosemicarbazone studies is their insolubility in different organic solvents. Tertiary phosphines are known to play an important role in solubilizing Cu^I complexes of heterocyclic thioamides.¹⁴ In this paper, the complexes of copper(I) halides with a series of thiosemicarbazone ligands (Scheme 1) in the presence of triphenylphosphine (Ph₃P) are reported. All of these have been characterized by elemental analysis, IR, ¹H, ¹³C, or ³¹P NMR spectroscopy, and X-ray crystallography. Ab initio density functional theory calculations have been carried out on model monomeric and dimeric complexes of the simplest thiosemicarbazone (H₂C=N–NH–C(S)–NH₂, Htsc) by considering its different coordination modes.

Experimental Section

General Materials and Techniques. Benzaldehyde, furan-2-carbaldehyde, pyridine-2-carbaldehyde, pyrrole-2-carbaldehyde, thiophene-2-carbaldehyde, and Ph₃P were procured from Aldrich Sigma Ltd. The ligands benzaldehyde thiosemicarbazone (Hbtsc),

furan-2-carbaldehyde thiosemicarbazone (Hftsc), pyridine-2-carbaldehyde thiosemicarbazone (Hpytsc), pyrrole-2-carbaldehyde thiosemicarbazone (Hptsc), and thiophene-2-carbaldehyde thiosemicarbazone (Httsc) were prepared by reported methods.¹¹ Copper(I) chloride, copper(I) bromide, and copper(I) iodide were prepared by the reduction of CuSO₄·5H₂O using SO₂ in the presence of NaCl, NaBr or iodide in water.¹⁵ The C, H, and N elemental analyses were obtained with a Carlo Erba 1108 microanalyzer from University of Santiago, Santiago, Spain. The melting points were determined with a Gallenkamp electrically heated apparatus. Infrared (IR) spectra were recorded using KBr pellets on a Pye Unicam SP-3-300 or Nicolet 320 Fourier transform IR spectrophotometer in the 4000–200 (or 400) cm⁻¹ range. ¹H NMR spectra of complexes were recorded on a JEOL AL-300 FT spectrometer operating at a frequency of 300 MHz in CDCl₃ with tetramethylsilane (TMS) as the internal reference. ¹³C NMR spectra of complexes were recorded on a JEOL AL-300 FT spectrometer operating at a frequency of 75.45 MHz using CDCl₃ as the solvent and TMS as the internal reference. ³¹P NMR spectra were recorded on a JEOL AL-300 FT spectrometer operating at a frequency of 121.5 MHz using CDCl₃ with *o*-phosphoric acid as the external reference.

[CuI(Hbtsc)(Ph₃P)₂] (1). To a solution of copper(I) iodide (0.025 g, 0.131 mmol) in acetonitrile (20 mL) was added solid Hbtsc (0.023 g, 0.131 mmol), and the contents were stirred for 4 h, followed by the addition of solid Ph₃P (0.064 g, 0.262 mmol) and continued stirring for another 1 h. The clear solution formed was filtered and allowed to evaporate at room temperature, and upon evaporation, a yellow crystalline product was formed (0.066 g, 56%; mp 218–222 °C). Anal. Calcd for C₄₄H₃₉CuI₂N₃P₂S: C, 59.1; H, 4.39; N, 4.69. Found: C, 59.5; H, 4.42; N, 4.76. Crystals were grown from an acetonitrile solution at room temperature. Main IR peaks (KBr, cm⁻¹): ν(N–H) 3446m, 3230m (–NH₂ group), 3126m (–NH–); ν(C–H) 3043m; δ(NH₂) + ν(C=N) + ν(C–C) 1580 (s), 1530s; ν(C=S) + ν(C–N) 1069s, 1026s, 815s (thioamide moiety); ν(P–C_{Ph}) 1093s. ¹H NMR data (δ, ppm; *J*, Hz; CD₃CN): 10.40 (s, N²H), 8.11 (s, C²H), 7.27 (s, br, N¹H₂), 7.78 (m, 2H, C^{4,8}H), 7.38–7.46 (m, 30H, Ph). ¹³C NMR data (δ, ppm; *J*, Hz; CDCl₃): 174.9 (C¹), 145.6 (C²), 134.3 (C³), 130.7 (C⁶), 129.2 (C^{4,8}), 127.6 (C^{5,7}), 133.1 (*i*-C, PhP), 133.9 (*o*-C, *J*_{P–C} = 28.3, PhP), 128.2 (*m*-C, *J*_{P–C} = 8.2, PhP), 128.8 (*p*-C, PhP).

[CuBr(η¹-S-Hbtsc)(Ph₃P)₂]·CH₃CN (2). Yield: yellow, 0.082 g, 56%. Mp: 118–120 °C. Elem anal. Calcd for C₄₆H₄₂CuBrN₄P₂S: C, 62.2; H, 4.77; N, 6.30. Found: C, 62.4; H, 4.88; N, 6.16. Crystals were grown from an acetonitrile solution at room temperature. Main IR peaks (KBr, cm⁻¹): ν(N–H) 3425m, 3319m (–NH₂), 3134m (–NH–); ν(C–H) 3053m, 2925m, 2853m; δ(NH₂) + ν(C=N) + ν(C–C) 1596s, 1539s, 1513s; ν(C=S) + ν(C–N) 1070s, 1027s, 818s (thioamide moiety); ν(P–C_{Ph}) 1094s. ¹H NMR data (δ, ppm; *J*, Hz; CDCl₃): 12.09 (s, br, N²H), 8.18 (s, C²H), 6.90, 6.08 (d, br, N¹H₂), 7.62 (m, 2H, C^{4,8}H), 7.24–7.42 (m, 30H, Ph). ¹³C NMR data (δ, ppm; *J*, Hz; CDCl₃): 175.1 (C¹), 146.4 (C²), 133.7 (C³), 130.5 (C⁶), 128.7 (C^{4,8}), 127.6 (C^{5,7}), 133.9 (*o*-C, *J*_{P–C} = 14.4, PhP), 128.2 (*m*-C, *J*_{P–C} = 9.1, PhP), 129.5 (*p*-C, PhP).

[Cu₂(μ-Br)₂(η¹-S-Hbtsc)₂(Ph₃P)₂] (3). To a solution of copper(I) bromide (0.025 g, 0.174 mmol) in CH₃CN (20 mL) was added solid Hbtsc (0.031 g, 0.174 mmol), and the contents were stirred for 4 h, and then solid Ph₃P (0.045 g, 0.174 mmol) was added. The stirring was continued for a further period of 1 h. The clear yellow-colored solution formed was filtered and allowed to evaporate at room temperature. Upon evaporation, a yellow

- (8) (a) Easmon, J.; Puringer, G.; Heinisch, G.; Roth, T.; Fiebig, H. H.; Holzer, W.; Jager, W.; Jenny, M.; Hofmann, J. *J. Med. Chem.* **2001**, *44*, 2164. (b) Lewis, J. S.; Easmon, J.; Rutlin, J. R.; Jones, L. A.; Welch, M. J. *J. Labelled Compd. Radiopharm.* **2003**, *46*, S388.
- (9) De Lima, R. L.; Teixeira, L. R. D.; Carneiro, T. M. G.; Beraldo, H. *J. Braz. Chem. Soc.* **1999**, *10*, 184.
- (10) Joshi, S. K.; Kumawat, R. C.; Shrivastava, B. D.; Nayak, A.; Pandeya, K. B. *Natl. Acad. Sci. Lett. (India)* **1996**, *19*, 236.
- (11) Akinchan, N. T.; Akinchan, R.; Drozdowski, P. M.; Yang, Y. H.; Klein, T. L.; West, D. X. *Synth. React. Inorg. Met.-Org. Chem.* **1996**, *26*, 1735.
- (12) (a) Zheng, H. G.; Zeng, D. X.; Xin, X. Q.; Wong, W. T. *Polyhedron* **1997**, *16*, 3499. (b) Lhuachan, S.; Siripaisarnpipat, S.; Chaichit, N. *Eur. J. Inorg. Chem.* **2003**, 263.
- (13) (a) Ashfield, L. J.; Cowley, A. R.; Dilworth, J. R.; Donnelly, P. S. *Inorg. Chem.* **2004**, *43*, 4121. (b) Cowley, A. R.; Dilworth, J. R.; Donnelly, P. S.; Labisbal, E.; Sousa, A. *J. Am. Chem. Soc.* **2002**, *124*, 5270. (c) Belicchi-Ferrari, M.; Gasparri-Fava, G.; Lanfranchi, M.; Pelizzi, C.; Tarasconi, P. *Inorg. Chim. Acta* **1991**, *181*, 253. (d) Belicchi-Ferrari, M.; Bonardi, A.; Gasparri-Fava, G.; Pelizzi, C.; Tarasconi, P. *Inorg. Chim. Acta* **1994**, *223*, 77. (e) Lobana, T. S.; Rekha; Sidhu, B. S.; Castineiras, A.; Bermejo, E.; Nishioka, T. *J. Coord. Chem.* **2005**, *58*, 803.
- (14) Lobana, T. S.; Castineiras, A. *Polyhedron* **2002**, *21*, 1603 and references cited therein.

- (15) Brauer, G. *Handbook of Preparative Chemistry*, 2nd ed.; Academic Press: New York, 1965; Vol. 2.

crystalline product was formed (0.055 g, 54%, mp 206–208 °C). Anal. Calcd for $C_{52}H_{48}Cu_2Br_2N_6P_2S_2$: C, 53.4; H, 4.14; N, 7.18. Found: C, 52.9; H, 4.21; N, 7.14. Crystals were grown from an acetonitrile solution at room temperature. Main IR peaks (KBr, cm^{-1}): $\nu(N-H)$ 3440m, 3260m ($-NH_2$), 3180 m ($-NH-$); $\nu(C-H)$ 3090(m); $\delta(NH_2) + \nu(C=N) + \nu(C-C)$ 1580s, 1530s; $\nu(C=S) + \nu(C-N)$ 1060s, 1029w, 803s (thioamide moiety); $\nu(P-C_{Ph})$ 1090s. 1H NMR data (δ , ppm; J , Hz; CD_3CN): 11.30 (s, br, N^2H), 8.19 (s, C^2H), 7.58 (s, br, N^1H_2), 7.62 (m, 2H, $C^{4,8}H$), 7.35–7.50 (m, 15H, Ph). ^{13}C NMR data (δ , ppm; J , Hz; $CDCl_3$): 147.7 (C^2), 132.4 (C^3), 131.1 (C^6), 129.8 ($C^{4,8}$), 127.86 ($C^{5,7}$), 132.8 ($i-C$), 133.9 ($o-C$, $J_{p-c} = 13.6$, PhP), 128.5 ($m-C$, $J_{p-c} = 12.3$, PhP), 128.8 ($p-C$, PhP).

Other dimers, **4** and **8–12**, were prepared similarly.

[Cu₂Cl₂(μ_2 -S-Hbtsc)₂(Ph₃P)₂] \cdot 2H₂O (4**)**. Yield: yellow, 0.088 g, 60%. Mp: 208–210 °C. Anal. Calcd for $C_{52}H_{52}Cu_2Cl_2N_6P_2S_2O_2$: C, 55.9; H, 4.66; N, 7.53. Found: C, 56.0; H, 4.74; N, 7.69. Crystals were grown from an acetonitrile solution at room temperature. Main IR peaks (KBr, cm^{-1}): $\nu(O-H)$ 3590s, 3510s; $\nu(N-H)$ 3416m, 3367s, 3200m ($-NH_2$); 3144s ($-NH-$); $\nu(C-H)$ 3075m, 3000w; $\delta(NH_2) + \nu(C=N) + \nu(C-C)$ 1597s, 1545s; $\nu(C=S) + \nu(C-N)$ 1061s, 1029m, 812s (thioamide moiety); $\nu(P-C_{Ph})$ 1094s. 1H NMR data (δ , ppm; J , Hz; $CDCl_3$): 12.33 (s, br, N^2H), 8.27 (s, C^2H), 7.11 (s, br, N^1H_2), 7.66 (m, 2H, $C^{4,8}H$), 7.30 (m, 2H, $C^{5-7}H$), 7.36–7.46 (m, 15H, Ph). ^{13}C NMR data (δ , ppm; J , Hz; $CDCl_3$): 174.3 (C^1), 147.8 (C^2), 132.6 (C^3), 130.9 (C^6), 129.8 ($C^{4,8}$), 127.7 ($C^{5,7}$); 132.6 ($i-C$), 134.6 ($o-C$, $J_{p-c} = 14.8$, PhP), 129.7 ($m-C$, $J_{p-c} = 11.5$, PhP), 128.8 ($p-C$, PhP).

[CuI(η^1 -S-Hpysc)(Ph₃P)₂] (5**)**. Yield: greenish-yellow, 0.069 g, 59%. Mp: 156–158 °C. Anal. Calcd for $C_{43}H_{38}CuIN_4P_2S$: C, 57.7; H, 4.28; N, 6.26. Found: C, 57.5; H, 4.19; N, 6.13. Crystals were grown from an acetonitrile solution at room temperature. Main IR peaks (KBr, cm^{-1}): $\nu(N-H)$ 3370m, 3269m, 3049m ($-NH-$), $\nu(C-H)$ 2925–2800mw; $\delta(NH_2) + \nu(C=N) + \nu(C-C)$ 1623s, 1586s, 1523s; $\nu(C=S) + \nu(C-N)$ 1067s, 1027s, 821s (thioamide moiety); $\nu(P-C_{Ph})$ 1093s. 1H NMR data (δ , ppm; J , Hz; $CDCl_3$): 8.05 (s, C^2H), 8.75 (t, 1H, C^7H), 8.25 (d, 1H, C^4H), 7.25–7.45 (m, 30H, Ph).

[CuBr(η^1 -S-Hpytsc)(Ph₃P)₂] (6**)**. Yield: yellow, 0.08 g, 58%. Mp: 170–172 °C. Anal. Calcd for $C_{43}H_{38}CuBrN_4P_2S$: C, 60.9; H, 4.52. Found: C, 60.9; H, 4.63. Crystals were grown from an acetonitrile solution at room temperature. Main IR peaks (KBr, cm^{-1}): $\nu(N-H)$ 3350–3280m, 3083m ($-NH-$); $\nu(C-H)$ 2970m; $\delta(NH_2) + \nu(C=N) + \nu(C-C)$ 1630s, 1578s, 1525s; $\nu(C=S) + \nu(C-N)$ 1080 m, 1015m, 820s (thioamide moiety); $\nu(P-C_{Ph})$ 1105s. 1H NMR data (δ , ppm; J , Hz; $CDCl_3$): 11.66 (s, br, N^2H), 8.23 (s, C^2H), 6.44 (s, br, N^1H_2), 8.67 (d, 1H, C^7H), 7.73 (d, 1H, C^4H), 7.27–7.44 (m, 30H, Ph).

[CuCl(η^1 -S-Hpytsc)(Ph₃P)₂] (7**)**. Yield: yellow, 0.12 g, 52%. Mp: 148–150 °C. Anal. Calcd for $C_{43}H_{38}CuClN_4P_2S$: C, 64.3; H, 4.73; N, 7.00. Found: C, 64.3; H, 4.55; N, 7.18. Crystals were grown from an acetonitrile solution at room temperature. Main IR peaks (KBr, cm^{-1}): $\nu(N-H)$ 3375s, 3265m, 3051m ($-NH-$); $\nu(N-H)$ 2925m; $\delta(NH_2) + \nu(C=N) + \nu(C-C)$ 1628s, 1589s, 1541s; $\nu(C=S) + \nu(C-N)$ 1070m, 1029m, 824s (thioamide moiety); $\nu(P-C_{Ph})$ 1092s. 1H NMR data (δ , ppm; J , Hz; $CDCl_3$): 12.6 (s, br, N^2H), 7.23, 7.18 (d, br, N^1H_2), 7.45–7.67 (m, 30H, Ph).

[Cu₂(μ -I)₂(η^1 -S-Hftsc)₂(Ph₃P)₂] (8**)**. Yield: yellow, 0.046 g, 57%. Mp: 218–220 °C. Anal. Calcd for $C_{48}H_{44}Cu_2I_2N_6O_2P_2S_2$: C, 46.3; H, 3.57; N, 6.75. Found: C, 45.9; H, 3.48; N, 6.94. Crystals were grown from an acetonitrile solution at room temperature. Main IR peaks (KBr, cm^{-1}): $\nu(N-H)$ 3419s, 3263m, 3176m ($-NH-$);

$\nu(C-H)$ 3020m; $\delta(NH_2) + \nu(C=N) + \nu(C-C)$ 1622s, 1581s, 1529s; $\nu(C=S) + \nu(C-N)$ 1069s, 1025m, 1016s, 816s (thioamide moiety); $\nu(P-C_{Ph})$ 1092s. 1H NMR data (δ , ppm; J , Hz; CD_3CN): 10.47 (s, br, N^2H), 7.98 (s, C^2H), 7.25 (s, br, N^1H_2), 6.90 (d, 1H, C^4H), 6.57 (dd, 1H, C^5H), 7.64 (d, 1H, C^6H), 7.33–7.47 (m, 15H, Ph).

[Cu₂Br₂(μ_2 -S-Hptsc)₂(Ph₃P)₂] \cdot 2H₂O (9**)**. Yield: yellow, 0.060 g, 62%. Mp: 180–182 °C. Anal. Calcd for $C_{48}H_{50}Br_2Cu_2N_8O_2P_2S_2$: C, 48.7; H, 4.26; N, 9.46. Found: C, 48.7; H, 4.20; N, 9.64. Main IR peaks (KBr, cm^{-1}): $\nu(O-H)$ 3553s; $\nu(N-H)$ 3394s, 3344s, 3236m ($-NH_2$), 3163m ($-NH-$), 3059m (NH, pyrrole); $\nu(C-H)$ 3001m; $\delta(NH_2) + \nu(C=N) + \nu(C-C)$ 1614s, 1591s, 1531s; $\nu(C=S) + \nu(C-N)$ 1069m, 1031s, 816s (thioamide moiety); $\nu(P-C_{Ph})$ 1095s. Crystals for X-ray study were grown from a CH_3CN solution.

[Cu₂Cl₂(μ_2 -S-Htptsc)₂(Ph₃P)₂] \cdot 2H₂O (10**)**. Yield: yellow, 0.080 g, 58%. Mp: 156–158 °C. Anal. Calcd for $C_{48}H_{50}Cu_2Cl_2N_8O_2P_2S_2$: C, 52.7; H, 4.57; N, 10.23. Found: C, 52.7; H, 4.62; N, 10.31. Crystals for X-ray study were grown from a CH_3CN solution. Main IR peaks (KBr, cm^{-1}): $\nu(O-H)$ 3575s; $\nu(N-H)$ 3398s, 3352s, 3200m ($-NH_2$), 3145m ($-NH-$), 3065m (NH, pyrrole); $\nu(C-H)$ 3000m; $\delta(NH_2) + \nu(C=N) + \nu(C-C)$ 1614s, 1593s, 1531s; $\nu(C=S) + \nu(C-N)$ 1065m, 1032s, 825s (thioamide moiety); $\nu(P-C_{Ph})$ 1094s. 1H NMR data (δ , ppm; J , Hz; $CDCl_3$): 11.58 (s, N^4H), 9.86 (s, br, N^2H), 8.02 (s, C^2H), 7.26 (s, br, N^1H_2), 6.93 (d, 1H, C^6H), 6.53 (d, 1H, C^4H), 6.21 (dd, 1H, C^5H), 7.37–7.61 (m, 15H, Ph).

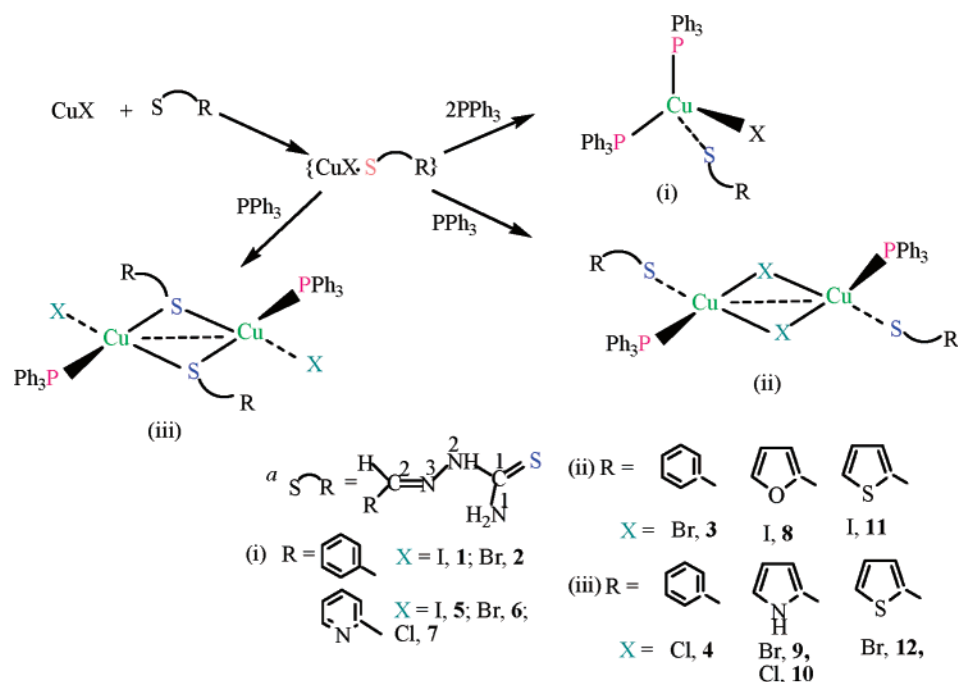
[Cu₂(μ -I)₂(η^1 -S-Httsc)₂(Ph₃P)₂] (11**)**. Yield: yellow, 0.060 g, 69%. Mp: 214–218 °C. Anal. Calcd for $C_{48}H_{44}Cu_2I_2N_6P_2S_4$: C, 45.2; H, 3.48; N, 6.58. Found: C, 45.6; H, 3.49; N, 6.62. Crystals were grown from an acetonitrile solution at room temperature. Main IR peaks (KBr, cm^{-1}): $\nu(N-H)$ 3396s, 3369s, 3205m ($-NH_2$), 3151m ($-NH-$); $\nu(C-H)$ 3065m; $\delta(NH_2) + \nu(C=N) + \nu(C-C)$ 1605m, 1581s, 1539s; $\nu(C=S) + \nu(C-N)$ 1069m, 1030s, 829s (thioamide moiety); $\nu(P-C_{Ph})$ 1095s. 1H NMR data (δ , ppm; J , Hz; $CDCl_3$): 11.5 (s, br, N^2H), 8.41 (s, C^2H), 7.14 (s, br, N^1H_2), 7.32 (d, 1H, C^4H), 7.03 (dd, 1H, C^5H), 7.41 (d, 1H, C^6H), 7.45–7.66 (m, 15H, Ph).

[Cu₂Br₂(μ_2 -S-Httsc)₂(Ph₃P)₂] \cdot 2H₂O (12**)**. Yield: yellow, 0.070 g, 65%. Mp: 190–192 °C. Anal. Calcd for $C_{48}H_{48}Br_2Cu_2N_6O_2P_2S_4$: C, 47.3; H, 3.97; N, 6.90. Found: C, 47.1; H, 3.92; N, 7.02. Crystals for X-ray study were grown from a CH_3CN solution. Main IR peaks (KBr, cm^{-1}): $\nu(O-H)$ 3582s, 3508m; $\nu(N-H)$ 3448s, 3392s, 3234m ($-NH_2$), 3159m ($-NH-$); $\nu(C-H)$ 3049m, 2831m; $\delta(NH_2) + \nu(C=N) + \nu(C-C)$ 1591s, 1550s; $\nu(C=S) + \nu(C-N)$ 1070m, 1030s, 827s (thioamide moiety); $\nu(P-C_{Ph})$ 1094s. 1H NMR data (δ , ppm; J , Hz; $CDCl_3$): 11.7 (s, br, N^2H), 8.44 (s, C^2H), 7.06 (dd, 1H, C^5H), 7.29–7.67 (m, 15H, Ph).

Results and Discussion

Synthesis and IR Spectroscopy. Scheme 2 shows the formation of copper(I) halide complexes with a series of thiosemicarbazone ligands and with Ph_3P as the coligand. Hbtsc formed monomers **1** and **2** and dimers **3** and **4**, Hpysc yielded monomers **5–7**, and Hftsc, Hptsc, and Httsc formed dimers **8–12**. Among the dimers, copper(I) iodide formed only iodide-bridged dimers (**8** and **11**), copper(I) chloride formed sulfur-bridged dimers (**4** and **10**), and copper(I) bromide formed both a bromine-bridged dimer (**3**) and sulfur-bridged dimers (**9** and **12**). Thus, all organic rings (R groups) give dimeric complexes with the exception of pyridine. In all of the complexes, thiosemicarbazones are acting as neutral

Scheme 2



S-donor ligands only (vide infra). The complexes studied are stable in air and moisture for several days. The soft Lewis bases (S donors) and Ph_3P (P donor) have a stabilized Cu^{I} state, which is otherwise susceptible to oxidation by air.

The IR spectra of the complexes show the presence of $\nu(\text{N-H})$ bands in the ranges $3490\text{--}3200\text{ cm}^{-1}$ ($-\text{NH}_2$ group) and $3126\text{--}3040\text{ cm}^{-1}$ ($-\text{NH}-$ group), and these data suggest that the thiosemicarbazone ligands are coordinating to a Cu center in the neutral form. Further, $\delta(\text{NH}_2)$, $\nu(\text{C}=\text{N})$, and $\nu(\text{C}=\text{C})$ vibrational modes appear in the range $1630\text{--}1513\text{ cm}^{-1}$, while the thioamide bands $\nu(\text{C}=\text{S}) + \nu(\text{C}-\text{N})$ appear in the range $1080\text{--}803\text{ cm}^{-1}$ (compared to free ligands, $1060\text{--}817\text{ cm}^{-1}$),¹⁶ and upon complexation, these shift to either lower energy, or higher energy, but the shifts are not significant. The appearance of characteristic $\nu(\text{P}-\text{C}_{\text{Ph}})$ bands at $1090\text{--}1105\text{ cm}^{-1}$ indicates the presence of Ph_3P in the complexes.

Structures of Complexes. Figures 1–4 depict structures of representative complexes: a monomer (**6**), a halogen-bridged dimer (**3**), and sulfur-bridged dimers (**4** and **9**), respectively. The important bond parameters for some complexes are given in Table 1. The complexes can be grouped into three isostructural classes: (i) monomers **1**, **2**, and **5–7** having S-bonded terminal ligands; (ii) halogen-bridged dimers, **3**, **8**, and **11**, with S-bonded terminal ligands, and (iii) sulfur-bridged dimers, **4**, **9**, **10**, and **12**, with terminal halogens (see the Supporting Information).

Monomers. A Cu atom of each monomer (**1**, **2**, and **5–7**) is coordinated to one S atom from a thiosemicarbazone and one halogen atom and two P atoms from two PPh_3 ligands. The Cu–S and Cu–P bond distances lie in the ranges $2.341\text{--}2.414$ and $2.272\text{--}2.305\text{ \AA}$, respectively (Table 1),

while the Cu–halogen bond distances lie in ranges $2.661\text{--}2.688$ (Cu–I), $2.489\text{--}2.548$ (Cu–Br), and 2.410 \AA (Cu–Cl). All of these bond distances are similar to those observed in the literature.^{12–14} The Cu–halogen bond distances are much less than the sum of the ionic radii of Cu and halogen (Cu^+ , I^- , 2.97 \AA ; Cu^+ , Br^- , 2.73 \AA ; Cu^+ , Cl^- , 2.58 \AA).^{17,18} The S–C bond distances lie in the range $1.64\text{--}1.71\text{ \AA}$ and are close to those ($1.66\text{--}1.72\text{ \AA}$) observed in $[\text{CuX}(\text{4-H}_2\text{-stsc})(\text{Ph}_3\text{P})_2]$ ($\text{X} = \text{Br}, \text{I}$)¹² and shorter than those observed in Hg^{II} complexes.¹⁶ The bond angles around a Cu atom lie in the range of ca. $102\text{--}123^\circ$ for the monomers, with the P–Cu–P bond angle being the largest (ca. $112\text{--}123^\circ$), and the S–Cu–X angles are in range of ca. $105\text{--}115^\circ$. The angles around the Cu centers suggest a distorted tetrahedral geometry, and this distortion is in view of the stereochemical requirements of bulky PPh_3 ligands.^{19,20}

Dimers. In the halogen-bridged dimers **3**, **8**, and **11**, each Cu atom is bonded to one terminal P atom of Ph_3P , one S atom of a thiosemicarbazone, and two halogen atoms with the central kernel $\text{Cu}(\mu_2\text{-X})_2\text{Cu}$ ($\text{X} = \text{halogen}$). PPh_3 and S-bonded ligands occupy trans orientations across the central kernel. Similarly, in the sulfur-bridged dimers **4**, **9**, **10**, and **12**, each Cu is bonded to one halogen atom, one P atom, and two S atoms from two different thiosemicarbazone ligands bridging two Cu centers with the central kernel $\text{Cu}(\mu_2\text{-S})_2\text{Cu}$. PPh_3 and halogen ligands occupy trans orientations across the central kernel $\text{Cu}(\mu_2\text{-S})_2\text{Cu}$. This sulfur–sulfur bridging is similar to that of heterocyclic thioamide

(16) Lobana, T. S.; Sanchez, A.; Casas, J. S.; Castineiras, A.; Sordo, J.; Garcia-Tasende, M. S.; Vazquez-Lopez, E. M. *J. Chem. Soc., Dalton Trans.* **1997**, 4289.

(17) Huheey, J. E.; Keiter, E. A.; Keiter, R. L. *Inorganic Chemistry: Principles of Structure and Reactivity*, 4th ed.; Harper Collins College Publishers: New York, 1993.

(18) Andersen, F. E.; Duca, C. J.; Scudi, J. V. *J. Am. Chem. Soc.* **1951**, *73*, 4967.

(19) Lobana, T. S.; Bhatia, P. K.; Tiekink, E. R. T. *J. Chem. Soc., Dalton Trans.* **1989**, 749.

(20) Karagiannidis, P.; Aslanidis, P.; Kessissoglou, D. P.; Krebs, B.; Dartmann, M. *Inorg. Chim. Acta* **1989**, *156*, 47.

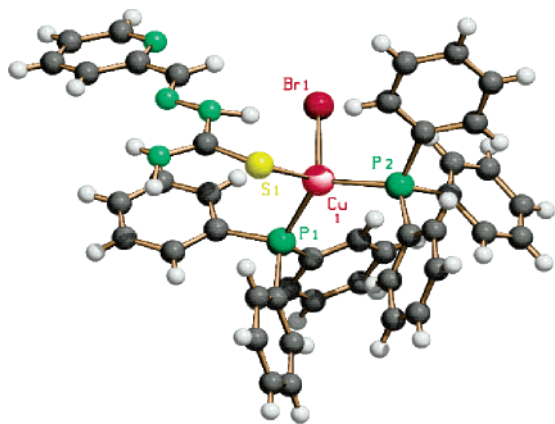


Figure 1. Structure of 6. Compounds 1, 2, 5, and 7 have similar structures.

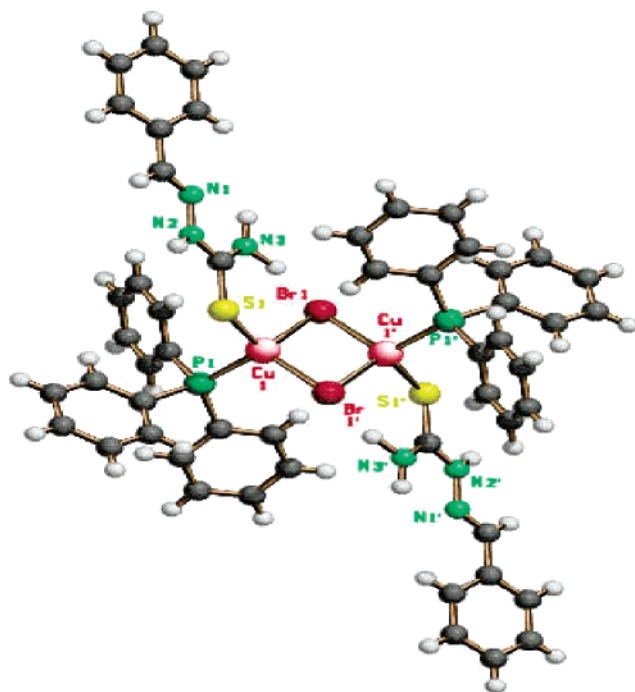


Figure 2. Structure of 3 with the numbering scheme. The symmetry operation indicated by the single prime is $(1 - x, -y, 1 - z)$. Dimers 8 and 11 have similar structures.

complexes of Cu^{I} with tertiary phosphines as coligands, which generally form sulfur-bridged dimers.¹⁴

The $\text{Cu}-\text{P}$ bond distances of the dimers lie in the range 2.231–2.261 Å, which are relatively short vis-à-vis those in monomers, and thus each PPh_3 ligand is more tightly bonded in dimers than in monomers. The $\text{Cu}-\text{S}$ bond distances lie in the range 2.331–2.344 Å for halogen-bridged dimers 3, 8, and 11 and in the range 2.366–2.410 Å for S-bridged dimers 4, 9, 10, and 12. In sulfur-bridged dimers (4 and 10), terminal $\text{Cu}-\text{Cl}$ bond distances ($\text{Cu}-\text{Cl}$, 2.328–2.359 Å) are short relative to that in monomer 7; however, terminal $\text{Cu}-\text{Br}$ bond distances, 2.478–2.485 Å (9 and 12), and bridging $\text{Cu}-\text{Br}$ bond distances, 2.485–2.579 Å (3), are comparable to those in monomers (2 and 5). Except one bridging $\text{Cu}-\text{I}$ bond distance of 2.817 Å of 11, other distances, 2.644–2.707 Å of 8 and 11, are comparable to those for monomers. The $\text{S}-\text{C}$ distances lie in the range

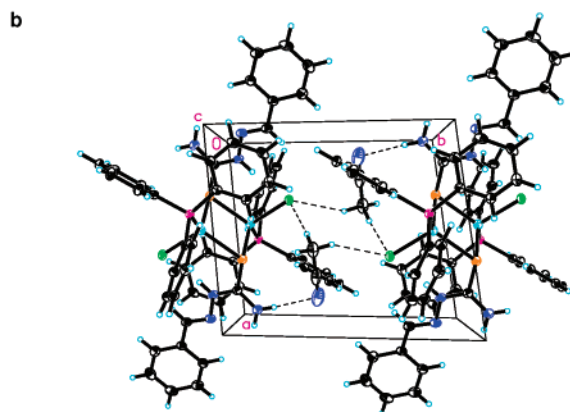
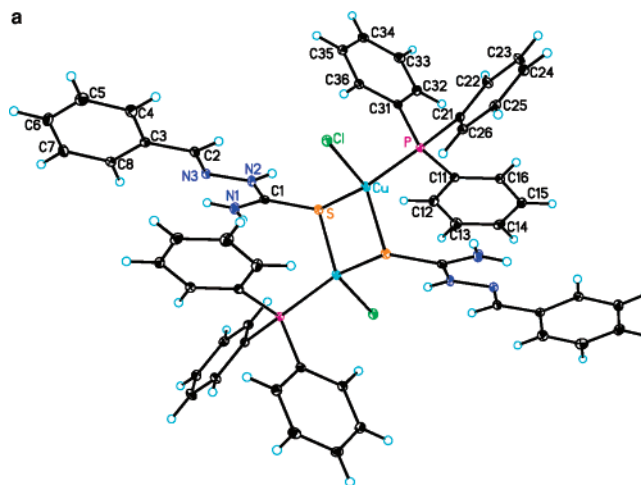


Figure 3. (a) Structure of 4. (b) Packing view of 4.

1.686–1.727 Å and are close to those (1.66–1.72 Å) observed in the literature.¹²

The geometry around each Cu center of dimers is distorted tetrahedral, with angles around it being ca. 102–119°. Two tetrahedra share halogen–halogen (3, 8, and 11) or sulfur–sulfur (4, 9, 10, and 12) edges. The central kernels $\text{Cu}(\mu_2\text{-X})_2\text{Cu}$ and $\text{Cu}(\mu_2\text{-S})_2\text{Cu}$ form parallelograms with unequal $\text{Cu}-\text{X}$ and $\text{Cu}-\text{S}$ bond distances, though the differences in some cases are small. The $\text{Cu}-\text{X}-\text{Cu}$ bond angles lie in the range of ca. 67–74° and, likewise, $\text{X}-\text{Cu}-\text{X}$ angles lie in the range 105–112°. Similarly, $\text{Cu}-\text{S}-\text{Cu}$ and $\text{S}-\text{Cu}-\text{S}$ bond angles lie in the ranges 72–84° and 95–107°, respectively. It was noted that the variations within the $\text{Cu}(\mu_2\text{-S})_2\text{Cu}$ cores are more significant than those in the $\text{Cu}(\mu_2\text{-X})_2\text{Cu}$ cores of dimers 3, 4, and 8–10 lie in the range 2.813–3.097 Å, while dimers 11 and 12 showed the largest values of 3.2247(6) and 3.2329(8) Å, respectively. The related dimers $[\text{Cu}_2\text{X}_2(\mu_2\text{-S}-\text{C}_5\text{H}_5\text{NS})_2(\text{PR}_3)_2]$ ($\text{C}_5\text{H}_5\text{NS}$ = pyridine-2-thione, $\text{R} = \text{Ph}$, *p*-tolyl, $\text{X} = \text{Br}$, I) showed $\text{Cu}\cdots\text{Cu}$ separations of 3.250–3.420 Å.^{14,21} The $\text{Cu}\cdots\text{Cu}$ separation is 3.226(6) Å within six-membered rings (Cu_3S_3) of $[\text{Cu}_6(\text{Hstsc})_6]$, and it is 2.850(2) Å between rings (Hstsc = uninegative anion of 2-salicylaldehyde thiosemicarbazone, N^2,S -bridging-cum-S-bridging).^{13a} The $\text{Cu}-\text{S}$ distances of

(21) Lobana, T. S.; Paul, S.; Castinerias, A. *Polyhedron* 1997, 16, 4023.

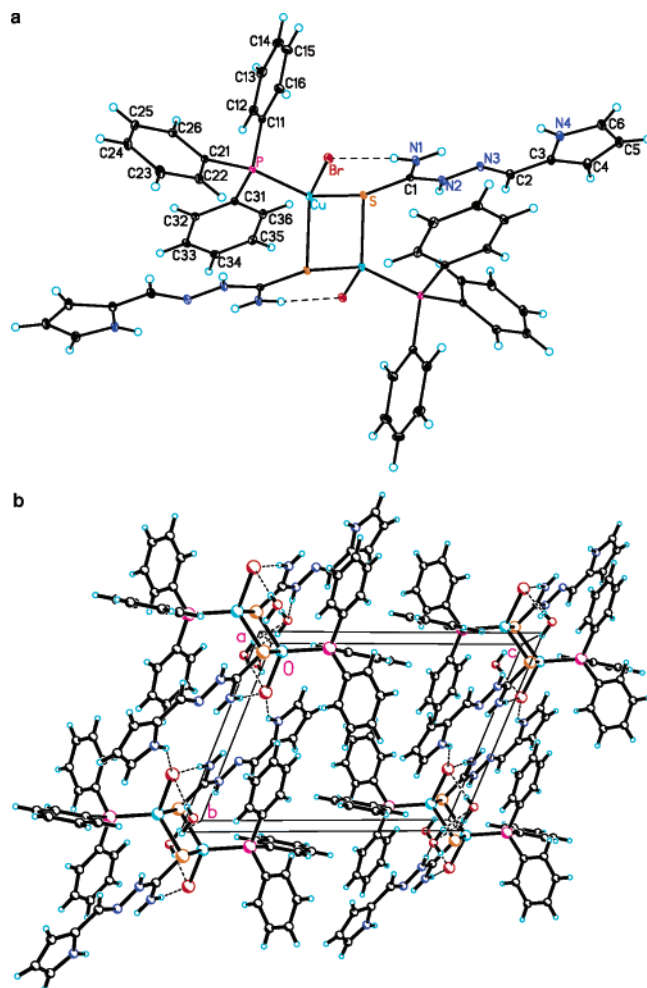


Figure 4. (a) Structure of **9**. (b) Packing diagram of **9**. Compounds **10** and **12** have similar structures.

2.240(1) and 2.251(1) Å in the Cu_3S_3 rings of hexanuclear cluster $[\text{Cu}_6(\text{Htsc})_6]^{13a}$ are short vis-à-vis those found for dimers or monomers as described above.

Hydrogen Bonding. In the solid state, both imino ($-\text{N}^2\text{H}-$) hydrogen and amino ($-\text{HN}^1\text{H}$) hydrogen atoms of thiosemicarbazones are involved in hydrogen bond formation in the monomers and dimers. In addition, the solvents of crystallization present are also involved in hydrogen bonding in **4**, **9**, **10**, and **12**. Chart 1 exhibits how the imino and amino hydrogen atoms are involved in hydrogen bond formation with halogens. Monomers **1**, **2**, and **5–7** exhibit $-\text{N}^2\text{H}\cdots\text{X}$ and $-\text{HN}^1\text{H}\cdots\text{X}$ bonds, while all dimers (**3** and **8–12**) except **4** have shown $-\text{HN}^1\text{H}\cdots\text{X}$ bonds. Monomers **1** and **2** exhibit intermolecular $-\text{HN}^1\text{H}\cdots\text{X}$ ($\text{X} = \text{I}, \text{Br}$) hydrogen bonding, leading to the formation of H-bonded dimers. In compound **2**, CH_3CN is lying as a lattice solvent with very weak contacts with the $\text{P}-\text{Ph}$ rings, viz., $\text{C}-\text{H}_{\text{Ph}}\cdots\text{NCCH}_3$. There are no intermolecular interactions in monomers **5** and **6** and dimers **3**, **8**, **11**, and **12**. Compound **7** involves intermolecular hydrogen bonds: $-\text{HN}^1\text{H}\cdots\text{N}^4_{\text{py}}$ and $\text{C}-\text{H}_{\text{py}}\cdots\text{Cl}$ form a dimer, and this dimer is further engaged in intermolecular $\text{C}-\text{H}_{\text{Ph}}\cdots\text{Cl}$ bonds involving $\text{P}-\text{Ph}$ rings with a third monomer. **7** may be regarded as a hydrogen-bonded trimer. CH_3CN is lying as a lattice solvent with no close contact.

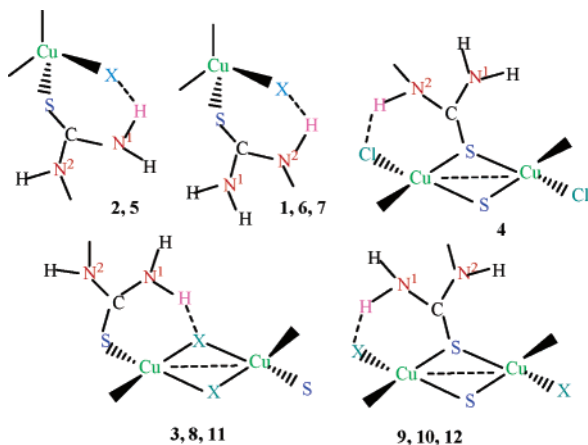
Table 1. Bond Lengths (Å) and Angles (deg) for Representative Compounds^a

[CuI(η^1 -S-Hbtsc)(Ph_3P) ₂] (1)			
Cu–P	2.3005(4)	Cu–P	2.2998(5)
Cu–S	2.339(1)	Cu–I	2.6889(3)
S–C	1.637(3)		
P–Cu–P	118.116(2)	P–Cu–I	103.924(14)
P1–Cu–S	110.08(2)	P–Cu–I	104.23(16)
P1–Cu–S	105.37(2)	Cu–S–C ^b	115.73(7)
S–Cu–I	115.42(2)		
[Cu ₂ (μ -Br) ₂ (η^1 -S-Hbtsc) ₂ (Ph_3P) ₂] (3)			
Cu–P	2.2343(13)	Cu–S	2.3443(12)
Cu–Br	2.5758(7)	Cu–Br*	2.4851(8)
Cu–Cu*	3.0543(11)	S–C8	1.686(4)
Cu*–Br–Cu	74.22(2)	Br*–Cu–Br	105.78(2)
P–Cu–S	111.37(5)	P–Cu–Br*	115.82(4)
S–Cu–Br*	103.01(4)	P–Cu–Br	106.36(4)
S–Cu–Br	114.65(4)	Cu–S–C8 ^b	112.41(16)
[Cu ₂ Cl ₂ (μ ₂ -S-Hbsc) ₂ (Ph_3P) ₂] \cdot 2CH ₃ CN (4)			
Cu–P	2.2309(6)	Cu–S	2.3662(6)
Cu–Cl	2.3280(6)	Cu–S*	2.4098(6)
Cu \cdots Cu*	2.8131(5)	S–C	1.716(2)
Cu–S–Cu	72.167(17)	P–Cu–S	107.15(2)
S–Cu–S*	107.833(17)	P–Cu–S*	118.76(2)
Cl–Cu–S	112.08(2)	Cl–Cu–P	110.12(2)
Cl–Cu–S*	100.89(2)	Cu–S–C ^b	110.54(7)
		Cu*–S–C ^b	104.08(7)
[CuBr(η^1 -S-Hpytsc)(Ph_3P) ₂] (6)			
Cu–P	2.2995(13)	Cu–P	2.2785(14)
Cu–S	2.4142(13)	Cu–Br	2.5475(8)
S–C	1.690(5)		
P2–Cu–P1	122.39(5)	P1–Cu–S	104.22(5)
P2–Cu–S	110.24(5)	P1–Cu–Br	106.40(4)
P2–Cu–Br	105.11(4)	S–Cu–Br	107.76(4)
Cu–S–C ^b	105.82(15)		
[Cu ₂ Br ₂ (μ ₂ -S-Hptsct) ₂ (Ph_3P) ₂] \cdot 2H ₂ O (9)			
Cu–P	2.2398(6)	Cu–Br	2.4851(4)
Cu–S	2.3769(6)	Cu \cdots Cu*	3.0087(5)
Cu–S*	2.4039(6)	S–C	1.727(2)
Cu–S–Cu	77.998(18)	P–Cu–S	109.04(2)
S–Cu–S*	102.002(18)	P–Cu–S*	116.95(2)
Br–Cu–P	111.607(17)	Cu–S–C ^b	112.34(7)
Br–Cu–S	113.436(17)	Cu*–S–C ^b	104.26(6)
Br–Cu–S*	103.526(18)		

^a Asterisks indicate the centrosymmetric Cu, S, or halogen as the case may be. ^b The carbons represent carbon C1 as shown in Scheme 1 (structure **1a**, *E*).

Dimer **4** has two CH_3CN molecules per dimer unit that are engaged in hydrogen bonding with amino hydrogen ($-\text{HN}^1\text{H}\cdots\text{NCCH}_3$) and halogens ($\text{Cl}\cdots\text{H}-\text{CH}_2\text{CN}$), a behavior different from that in compounds **2** and **7**. As shown in the packing diagram (Figure 3b), this hydrogen bonding leads to the formation of chains along the *a* axis. Dimers **9** and **10** involve intermolecular $-\text{N}^4\text{H}_{\text{pyrrole}}\cdots\text{X}$ hydrogen bonding, leading to the formation of hydrogen-bonded tetramers (see the Supporting Information). Dimers **9**, **10**, and **12** each have two H_2O molecules that are engaged in hydrogen bonding with halogen atoms ($\text{HOH}\cdots\text{X}$); apart from hydrogen bonding with N^2H hydrogen (Figure 4b), dimers **4**, **9**, **10**, and **12** all showed the presence of H_2O , as revealed by elemental analysis, and X-ray crystallography showed its presence in **9**, **10**, and **12** except **4**, in which CH_3CN replaced H_2O because crystals had to be stored in this

Chart 1



solvent. In all of these four compounds, solvents of crystallization are involved in hydrogen bonding with halogens, thus stabilizing sulfur bridging.

Theoretical Modeling Studies. Using model thiosemicarbazone Htsc and tertiary phosphine (PH_3) ligands, the electronic structure calculations using the B3LYP/LanL2DZ method²² were carried out on tetrahedral complexes: $[\text{CuX}(\eta^1\text{-S-Htsc})(\text{PH}_3)_2]$ ($X = \text{Cl, Br, I}$; **13–15**) with unidentate S-bonded Htsc (see the Supporting Information). Another set of tetrahedral complexes, $[\text{CuX}(\eta^2\text{-N}^3\text{,S-Htsc})(\text{PH}_3)]$ ($X = \text{Cl, Br, I}$; **16–18**) with $\text{N}^3\text{,S}$ -chelating Htsc, were also considered. The ab initio calculations revealed that complexes **13–15** are more stable than complexes **16–18** by 22.02, 20.33, and 18.75 kcal/mol, respectively. The greater thermodynamic stability of **13–15** (no chelation) over **16–18** (chelation) suggests that chelation by neutral Htsc in copper(I) halide complexes is not favored and Htsc ligands bind via thione S only in conformity with the experimental results (**1, 2, and 5–7**).

The structures of halogen-bridged dimers $[\text{Cu}_2(\mu\text{-X})_2(\text{Htsc})_2(\text{PH}_3)_2]$ ($X = \text{Cl, Br, I}$; **19–21**) were also optimized using B3LYP/LanL2DZ. Energy estimations suggested that both monomeric (**13–15**) and halogen-bridged dimeric (**19–21**) complexes have nearly similar stability. Attempts to identify the sulfur-bridged dimers on the respective potential energy surfaces using the B3LYP/LANL2DZ method were unsuccessful, revealing that sulfur-bridged dimers for copper(I) halides are not possible with thiosemicarbazone ligands,

which is in contradiction with the experimental results (**4, 9, 10, and 12**). It is possible that other factors such as the presence of solvent of crystallization, engaged in a network of hydrogen bonds, may be instrumental in this difference in the theoretical and experimental results. To understand the factors stabilizing the formation of sulfur-bridged complexes, calculations on the S-bridged analogues of **19–21** were repeated using two H_2O molecules, forming hydrogen bonds with halogens. As expected, the sulfur-bridged dimeric structures (**22–24**), with two H_2O molecules each, could be successfully identified as local minima on the potential energy surface. When H_2O was removed from **22–24** and reoptimized, the structures collapsed. Thus, it became apparent that hydrogen bonding between solvent molecules and halogen atoms of dimers is playing an important role in the formation of sulfur-bridged dimers **4, 9, 10, and 12**.

NMR Spectroscopy. The ^1H NMR spectra of sparingly soluble complexes in CDCl_3 (or in acetonitrile) reveal the presence of hydrazinic N^2H protons in the range of ca. δ 9.50–12.50 ppm (cf. Scheme 1 for numbering), and the signals are generally at low field vis-à-vis free ligands, which suggests that thiosemicarbazones are coordinating to Cu as neutral ligands, probably via S-donor atoms only (cf. the Experimental Section). Further, the N^1H_2 protons show two signals (due to restricted rotation of the NH_2 group along the C1–N1 bond of thioamide) in the range δ 6.60–8.06 ppm in ligands,¹⁶ and in the complexes, these appear in the altered positions at ca. δ 6.00–8.40 ppm. Except compound **2**, all other complexes showed only one broad band for N^1H_2 protons, and a second band is probably obscured by protons of phenyl or heterocyclic rings. It may be noted that, in the deprotonated form, $^1\text{NH}_2$ signals appear as a single band, e.g., $[\text{PhHg}(\text{btsc})]$.¹⁶ The azomethine C^2H protons of the complexes show an irregular trend; for example, complexes **1–4** showed upfield shifts, while other complexes, **5–8** and **10–12**, showed downfield shifts relative to the free ligands. Not all of the ring protons (R) of thiosemicarbazones could be located in the complexes (some obscured by PPh_3 protons), which, however, are not much affected.

The ^{13}C NMR spectra of complexes **1, 2, and 4** showed signals for ^{13}C carbons at δ 174.9, 175.1, and 174.3 ppm, respectively, which are upfield vis-à-vis free ligand (δ 178.9 ppm).¹⁶ The ^{29}Si carbon signals at δ 145.6 (**1**), 146.4 (**2**), and 147.8 (**4**) ppm are at low field relative to the free ligand (δ 143.9 ppm).¹⁶ This behavior is similar to that observed for phenylmercury(II) thiosemicarbazone complexes.¹⁶ For complex **3**, the ^{13}C carbon signal could not be detected, and the ^{29}Si carbon signal appeared at δ 147.7 ppm, which is upfield relative to the free ligand (δ 143.9 ppm).¹⁶ Further, the ring carbon signals do not show any significant shifts upon complexation, but the *i*-C, *o*-C, *m*-C, and *p*-C signals of Ph_3P are clearly resolved in the complexes.

The ^{31}P NMR spectra of monomers $\text{CuX}(\text{Htsc})(\text{PPh}_3)_2$, **1, 2, and 5** in CDCl_3 with terminally S-bonded thiosemicarbazones showed one signal each at δ_{P} 23.2, 24.3, and 24.4 ppm, respectively (Table 2).²¹ On the other hand, the sulfur-bridged dimer **10** gave a signal at δ_{P} 58.2 ppm. Iodide-bridged dimer **11** exhibits one signal at δ_{P} 58.9 ppm similar to that shown

(22) (a) Parr, R. G. *Density Functional Theory of Atoms and Molecules*; Oxford University Press: New York, 1989. (b) Lee, C.; Yang, W.; Parr, R. G. *Phys. Rev. B* **1988**, *37*, 785. (c) Becke, A. D. *J. Chem. Phys.* **1993**, *98*, 5648. (d) Hay, P. J.; Wadt, W. R. *J. Chem. Phys.* **1985**, *82*, 299. (e) Frisch, M. J.; Trucks, G. W.; Schlegel, H. B.; Scuseria, G. E.; Robb, M. A.; Cheeseman, J. R.; Zakrzewski, V. G.; Montgomery, J. A.; Stratmann, R. E., Jr.; Burant, J. C.; Dapprich, S.; Millam, J. M.; Daniels, A. D.; Kudin, K. N.; Strain, M. C.; Farkas, O.; Tomasi, J.; Barone, V.; Cossi, M.; Cammi, R.; Mennucci, B.; Pomelli, C.; Adamo, C.; Clifford, S.; Ochterski, J.; Petersson, G. A.; Ayala, P. Y.; Cui, Q.; Morokuma, K.; Malick, D. K.; Rabuck, A. D.; Raghavachari, K.; Foresman, J. B.; Cioslowski, J.; Ortiz, J. V.; Baboul, A. G.; Stefanov, B. B.; Liu, G.; Liashenko, A.; Piskorz, P.; Komaromi, I.; Gomperts, R.; Martin, R. L.; Fox, D. J.; Keith, T.; Al-Laham, M. A.; Peng, C. Y.; Nanayakkara, A.; Gonzalez, C.; Challacombe, M.; Gill, P. M. W.; Johnson, B.; Chen, W.; Wong, M. W.; Andres, J. L.; Gonzalez, C.; Head-Gordon, M.; Replogle, E. S.; Pople, J. A. *Gaussian 98*; Gaussian, Inc.: Pittsburgh, PA, 1998.

Table 2. ^{31}P NMR Data of Complexes (δ , ppm)

compound	δ_{P}	$\Delta\delta^a$	compound	δ_{P}	$\Delta\delta$
1	23.2	30.9	7	58.4, 25.4	66.1; 33.1
2	24.3	32.0	8	23.6	31.3
3	23.3	31.0	9	insoluble	
4	25.7	33.4	10	58.2	65.9
5	24.4	32.1	11	58.9	66.6
6	-6.65	1.1	12	25.4	33.1

$$^a \Delta\delta = \delta_{\text{complex}} - \delta_{\text{ligand}}$$

by compound **10**, and this suggests isomerization to a sulfur-bridged dimer. The addition of 2 mol of PPh_3 to dimer **11** in an NMR cell gave a signal at δ_{P} 23.1 ppm, and this shows the conversion of dimer into monomer. The addition of 2 mol of PPh_3 to dimer **10** in an NMR cell gave two signals, one at δ_{P} 24.4 ppm and a second at δ_{P} 59.8 ppm, and this shows the formation of a monomer, $\text{CuCl}(\text{S-Hptsc})(\text{PPh}_3)_2$, in equilibrium with its dimer. The sulfur-bridged dimers **4** and **12** gave one signal each at $\delta_{\text{P}} = 25.7$ and 25.4 ppm, respectively, and this shows their conversion into monomers. The addition of 2 mol of PPh_3 to dimer **4** in an NMR cell marginally shifted the signal from δ_{P} 25.7 to 25.1 ppm, and this confirms the conversion of dimer into monomer. Monomer **7** gave two signals at δ_{P} 25.4 and 58.4 ppm instead of one, and this shows the presence of monomer–dimer (sulfur-bridged) equilibrium. Bromide- and iodide-bridged

dimers **3** and **8** showed signals (δ_{P} 23.3 and 23.6 ppm, respectively) in the region of monomers, and this supports their conversion into monomers. Monomer **6** showed one broad signal at high field ($\delta_{\text{P}} -6.65$ ppm), and this position is close to that of the free PPh_3 ligand ($\delta_{\text{P}} -7.71$ ppm),¹⁴ and from here, it is inferred that N^3 and N^4 nitrogens of Hpytsc probably exchange for PPh_3 ligands in CDCl_3 .

Conclusion. Thiosemicarbazones with copper(I) halides form S-bonded monomers, halogen-bridged dimers with terminal S bonding, and sulfur-bridged dimers with halogen in the terminal position. Hydrogen bonding due to solvent of crystallization with halogens is a prerequisite for stabilization of sulfur bridging. Theoretical and experimental data are in conformity with each other.

Acknowledgment. Financial help from the University Grants Commission New Delhi is gratefully acknowledged.

Supporting Information Available: X-ray methods, crystal data, bond parameters, X-ray figures of various complexes, and theoretical modeling studies. X-ray crystal data in CIF format. This material is available free of charge via the Internet at <http://pubs.acs.org>. CCDC numbers are 240782–240784, 256127, 240787, 240786, 256128, 240785, 256129, 256130, 256131, and 256132 for **1–12**, respectively.

IC051018J